

# Partial response maximum likelihood channels for perpendicular magnetic recording system using bit-patterned media

Yoshihiro Okamoto\*, Hiroyuki Sugai\*, Yasuaki Nakamura\*, Hisashi Osawa\*,  
Hiroaki Muraoka\*\*, Hajime Aoi\*\* and Yoshihisa Nakamura\*\*

**Abstract:** Partial response maximum likelihood (PRML) channels are studied in R/W channels using bit-patterned media. Bit error rate (bER) performance and error events of generalized PRML (GPRML) systems with a noise predictor are evaluated. The bER performance obtained by computer simulation shows that the GPR channel based on full-response channel shows good performance. In addition, the error events of GPRML systems in the R/W channel using double layered bit-patterned medium are compared with those of continuous medium, and it is clarified by the error event characteristics that the two kinds of R/W channels using bit-patterned and continuous media have quite different characteristics.

**Keywords:** Partial response maximum likelihood (PRML), bit-patterned medium, perpendicular magnetic recording

## 1. Introduction

Hard disk drive (HDD) has played a key role of information storage systems, and is expected as a primary storage device in our information society. The HDD has to increase the recording density continuously in order to respond to expectations from users, however, it has some problems to be solved.

Perpendicular magnetic recording (PMR) system using bit-patterned medium is paid attention as a candidate for next-generation of magnetic recording system to achieve areal densities of 1 Tera-bit per square inch (1 Tbps) and higher [1]. The bit-patterned media have an excellent recording potential for both thermal stability in high areal densities and suppression of transition noise, such as jitter-like medium noise [2], [3]. And the noise does not depend on the recorded signal. However, it is difficult to make and arrange the fine magnetic islands as tracks on the disk, and various fabrication methods for the bit-patterned medium are attempted [4].

Signal processing such as the partial response maximum likelihood (PRML) channel is also studied for the R/W channels using bit-patterned media [5]. We study on an application of PRML channels to PMR channels using bit-patterned media.

## 2. R/W Channel Model

The block diagram of a generalized PRML (GPRML) system with a R/W channel using a bit-patterned medium is illustrated in Fig.1. We evaluate the performance of PRML channels for R/W channels using two types of bit-patterned media composed of a double layered medium with a soft under layer (SUL) and a single layered medium without the SUL. The double layered medium which the islands are set in line is shown in Fig. 2 where  $L_i$  and  $L_b$  are an island length and a user bit interval, respectively, and  $L_i/L_b$  stands for the duty ratio ( $DR$ ) of an island.

The islands arranged in line are magnetized by a synchronized NRZ recording signal with the island period corresponding to recording data sequence with bit rate  $f_b$ . First, we consider R/W channel models of perpendicular

\*Graduate School of Science and Engineering, Ehime University, Matsuyama 790-8577

\*\*RIEC, Tohoku University, Sendai 980-8577

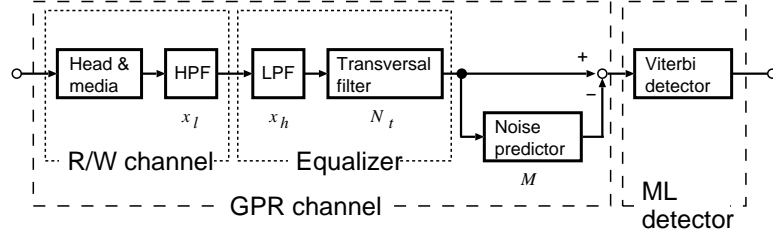


Fig. 1: Block diagram of GPRML system.

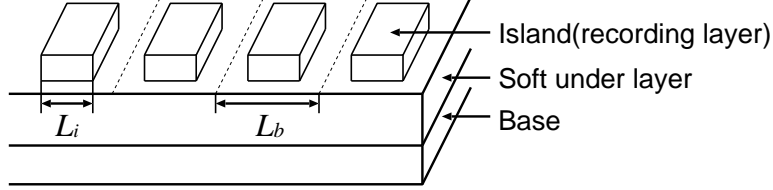


Fig. 2: Structure of double layered patterned media.

Table 1: Media and Head Parameters

Parameters	Patterned media	Continuous media
Magnetic spacing [nm]	5	5
Read gap [nm]	36	36
Thickness of the recording layer [nm]	13	13
Width of read element [nm]	18	36
Bit length [nm]	18	12.73

magnetic recording systems using bit-patterned media The two kinds of reproducing waveforms from the respective isolated lands with the infinite length are shown in Fig.3 where the symbols black circle and square show the levels of the waveforms readback from the double layered medium with SUL and the single layered medium without SUL, respectively. The respective waveforms are calculated at the parameters for the bit-patterned media shown in Table 1 [6], [7], and time  $t$  is normalized by  $T_b = 1/f_b = L_b/v$  where  $f_b$  and  $v$  are a user bit rate and a head-to-medium relative velocity, respectively.

The isolated waveforms readback from the land with an infinite length are normalized by the saturation level  $A$  of the waveform readback from the double layered medium. We define the time which the isolated waveform from the double layered medium needs to rise from  $A/4$  to  $3A/4$  as  $T_{50}$ , and the normalized linear density is defined as  $K_p = T_{50}/T_b$ . In Fig.3, the isolated waveform from the double layered medium at  $K_p = 0.56$  is shown with the waveform from the same land of the single layered medium without SUL. As can be seen from the figure, the amplitude of the reproducing waveform from the double layered medium is larger than that of the single layered. And the waveform from the single layered medium has overshoots, and while they are not so large.

We assume an additive white Gaussian noise (AWGN) as an electronic noise due to a pre-amplifier. When the power of AWGN fallen in the bandwidth of  $0.6f_b$  is expressed as  $\sigma_W^2$ , the SNR for the AWGN at the reading point is defined as

$$\text{SNR}_W = 20 \log_{10} A/\sigma_W \text{ [dB]}. \quad (1)$$

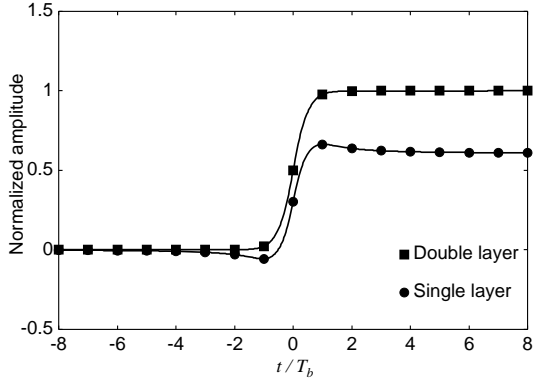


Fig. 3: Isolated waveforms from patterned media ( $K_p = 0.56$ ).

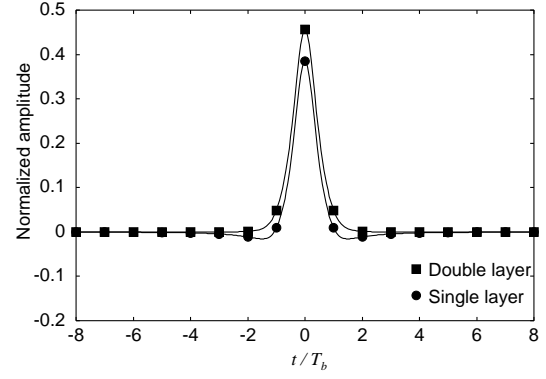


Fig. 4: Reproducing waveforms from isolated island ( $K_p = 0.56$ ).

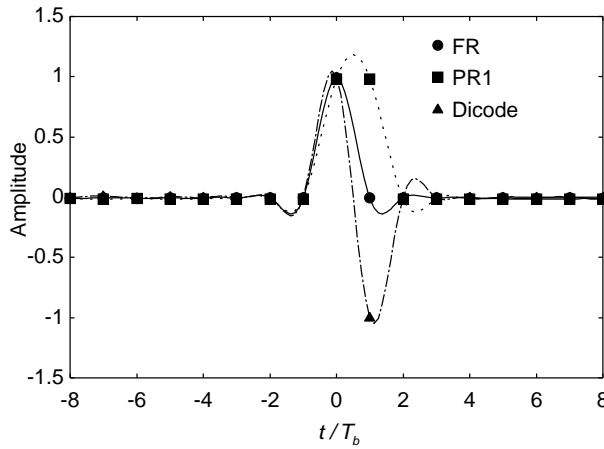


Fig. 5: Equalized waveforms of FR, PR1, and dicode channels ( $K_p = 0.56$ ,  $x_l = 3.0 \times 10^{-3}$ ,  $N_t = 15$ ,  $x_h = 0.4$ ).

And a transition jitter in the island edge is also assumed as a medium noise. Then, we assume that the transition jitter is caused by the fabrication condition for the respective islands, and the distribution of the jitter is followed by Gaussian distribution with a standard deviation  $\sigma_t$  normalized by the bit interval  $T_b$ .

The R/W channel involves a low-frequency cut-off due to pre-amplifier whose frequency normalized by  $f_b$  is  $x_l$ . The equalizer in Fig.1 is composed of a low-pass filter (LPF) with a normalized cut-off frequency  $x_h$  and a transversal filter with  $N_t$  taps. We consider the full-response (FR), PR1, and dicode channels as Fig.4 shows the reproduced waveforms from isolated islands at  $K_p = 0.56$ . The symbols are the same as those in Fig. 3. As the waveform from the double layered medium is larger than that from the single layered medium, the system using the double layered medium can have higher SNR for the AWGN in the pre-amplifier.

The characteristics of the equalizer is determined so as to form the reproducing waveforms into the required targets. The reproducing waveform from the double layered medium shown in Fig.4 is equalized as shown in Fig.5 where  $x_l = 3.0 \times 10^{-3}$ ,  $N_t = 15$  and  $x_h = 0.4$  are set as the parameter of the channel. The symbols black circle, square, and triangle in the figure show the waveforms of an FR channel, a PR1 channel, and a dicode channel, respectively. It is known that the reproducing waveform is good-equalized to the respective targets, and in the case of the single layered medium, the reproducing waveform from an isolated island shown by the symbol of circle in Fig.4 is similarly good-equalized.

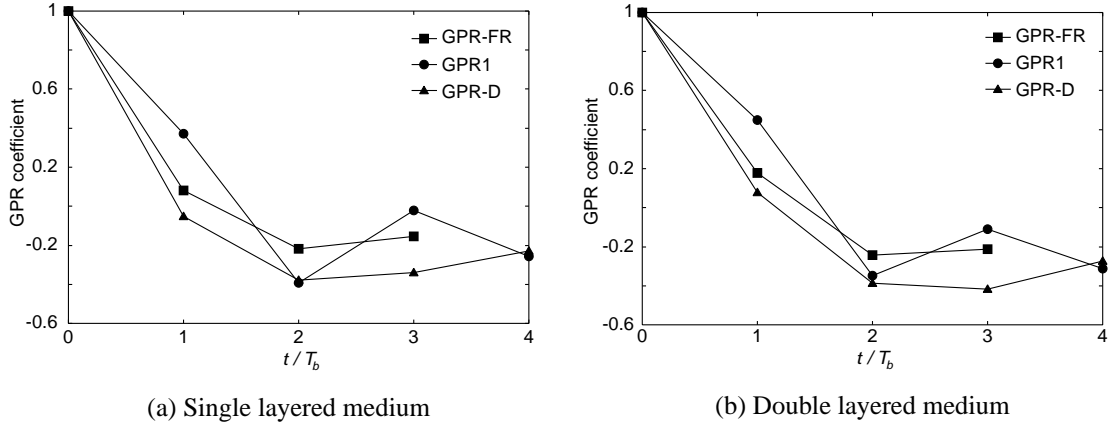


Fig. 6: Bit response of GPR channels ( $K_p = 0.56$ ,  $\sigma_t = 0$ ,  $\text{SNR}_w = 23\text{dB}$ ,  $x_l = 3.0 \times 10^{-3}$ ,  $x_h = 0.4$ ,  $N_t = 15$ ,  $M = 3$ ).

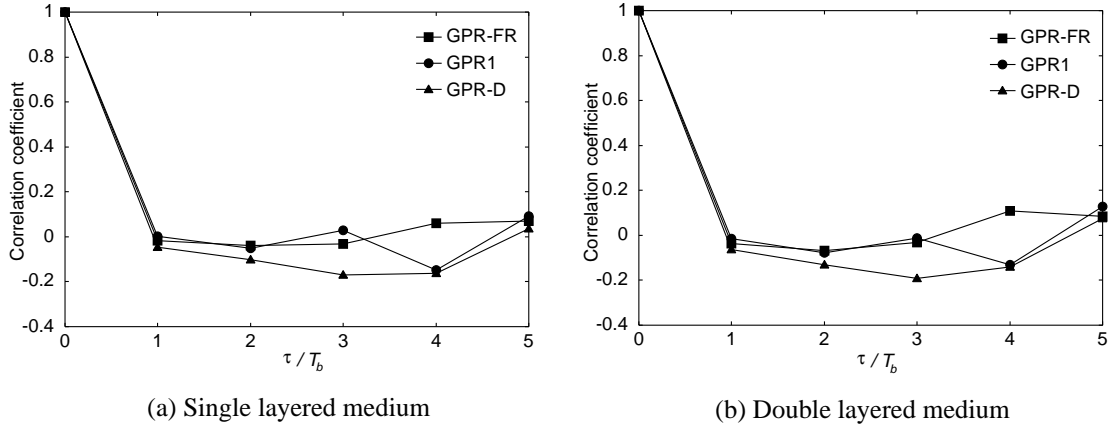


Fig. 7: Correlation coefficients of noise at GPR channel output ( $K_p = 0.56$ ,  $\sigma_t = 0$ ,  $\text{SNR}_w = 23\text{dB}$ ,  $x_l = 3.0 \times 10^{-3}$ ,  $x_h = 0.4$ ,  $N_t = 15$ ,  $M = 3$ ).

The equalized waveform is re-equalized to the GPR target by a noise predictor with  $M$  channel bit delays so that the noise at the output of GPR channel becomes white, or it does not have a correlation between the noise samples. Here, we can obtain the three kinds of GPR channels from the previous channels shown in Fig.5. Accordingly, the GPR channels are labeled as the GPR-FR, GPR1, and GPR-D channels so that the previously equalized targets are known from the notations. The output waveforms of GPR channels with  $M = 3$  are shown in Fig.6. (a) and (b) in the figure show the bit responses for the respective GPR channels in the case of single layered and double layered media, respectively. The symbols black circle, square, and triangle in the figure show the responses for the GPR-FR, GPR1, and GPR-D channels, respectively. The parameters of the channels are set as  $K_p = 0.56$ ,  $\sigma_t = 0$ ,  $\text{SNR}_w = 23\text{dB}$ ,  $x_l = 3.0 \times 10^{-3}$ ,  $x_h = 0.4$ ,  $N_t = 15$  and  $M = 3$ . In any GPR channel, each bit response extends compared with that of the first PR response to whiten the noise at the output of the equalizer in Fig.1. The bit responses of GPR channels are so different, though the waveform from an isolated island on the double layered medium shown in Fig.4 differs with that of the single layered medium.

Fig.7 shows the correlation coefficients of the noise at the output of GPR channel where, (a) and (b) also show the cases of the single layered and the double layered. The symbols are the same as Fig.6. From the figure, it can be seen that the noise sequences have a little correlation between noise samples in any obtained GPR channel,

or the noises are not completely white. Furthermore, the correlations of noises are also different in the respective GPR channels, however, they are not so different from the medium point of view.

The output sequence from the GPR channel is input to the Viterbi detector, and is decoded by the detector with  $2^M$  states for the GPR-FR channel, and  $2^{M+1}$  states for the GPR1 and GPR-D channel.

### 3. Performance Comparison

Fig.8 shows the bit error rate (bER) performance for the transition jitter where symbols squares, circles and triangles show the performances of the GPR-FRML, GPR1ML, and GPR-DML channels, respectively. The bERs are obtained by R/W simulation for  $10^6$  user bit sequence. The white and the black symbols show the cases of using the double and the single layered media. The parameters for the simulation are set as  $\text{SNR}_W=23\text{dB}$ ,  $DR = 0.5$ ,  $x_l = 3.0 \times 10^{-3}$ ,  $x_h = 0.4$ ,  $N_t = 15$ , and  $M = 3$ . The linear density  $K_p$  is also set as 0.56, which means the aerial density of 1 Tbps [6]. In the figure, the systems using the double layered media show the better performance compared with those of the single layered medium, and the GPR-FR systems show the most excellent performance among three GPRML systems.

Fig.9 shows the isolated reproducing waveform of a double layered perpendicular continuous medium at the reading point with that of the double layered bit-patterned media shown in Fig.3. The symbols black square and circle show the waveforms of the double layered bit-patterned and continuous media, respectively. The waveform from the continuous medium is also obtained from the parameters for an areal density of 1 Tbps shown in Table I [6], [7]. And the bit length  $L'_b$  is  $L_b/\sqrt{2}$  ( $= 12.73\text{nm}$ ) and the track pitch  $T'_p$  is  $\sqrt{2}T_p$  where  $T_p$  is the track pitch of the bit-patterned medium. The bit interval  $T_b$  for the continuous media equals that for patterned media, because the linear velocity  $v'$  of the continuous is set at  $v' = v/\sqrt{2}$ . The track width of the continuous media is twice as large as that of the bit-patterned medium. From the figure, it can be seen that the waveform of the continuous medium

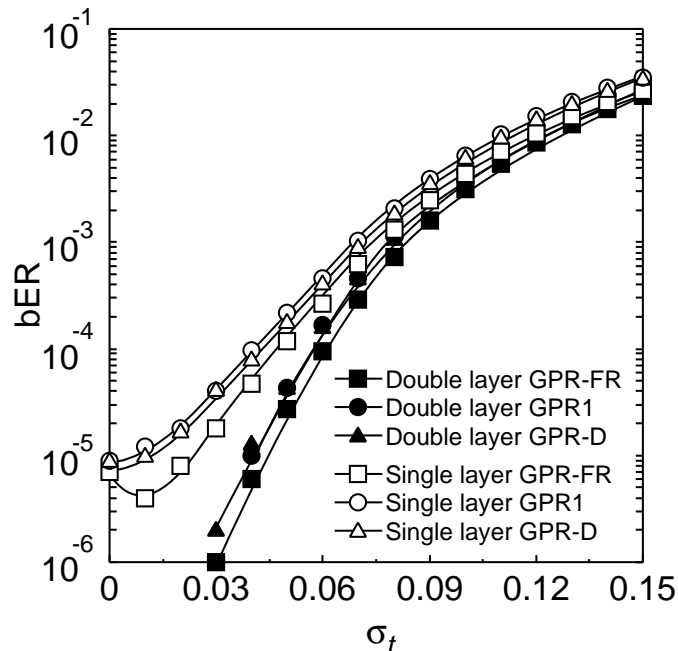


Fig. 8: bER performance of patterned media ( $\text{SNR}_W=23\text{dB}$ ,  $DR = 0.5$ ,  $x_l = 3.0 \times 10^{-3}$ ,  $x_h = 0.4$ ,  $N_t = 15$ ,  $M = 3$ ).

has a large saturation level  $A'$  compared with that of the bit-patterned medium. However, the normalized linear density of the continuous medium  $K_c = K'_p = 1.03$  is larger than that of the bit-patterned medium.  $T'_{50}$  is also the time which the waveform from the continuous medium needs to rise from  $-A'/2$  to  $A'/2$ . Fig. 10 shows the bER performance for the transition jitter. The performance of the patterned medium is the same as the performance shown Fig. 8. The symbol white circle shows the performance of GPR1ML channel in the case of the continuous medium at  $K_c = 1.03$ . It is seen from the figure that the R/W channel using the continuous medium can permit larger transition jitter. However, it is expected that the transition jitter in the channel using the patterned media is smaller than that of the continuous. If the transition jitter in the bit-patterned medium is less than half of that of the continuous medium, the system using the bit-patterned medium can obtain the performance improvement over

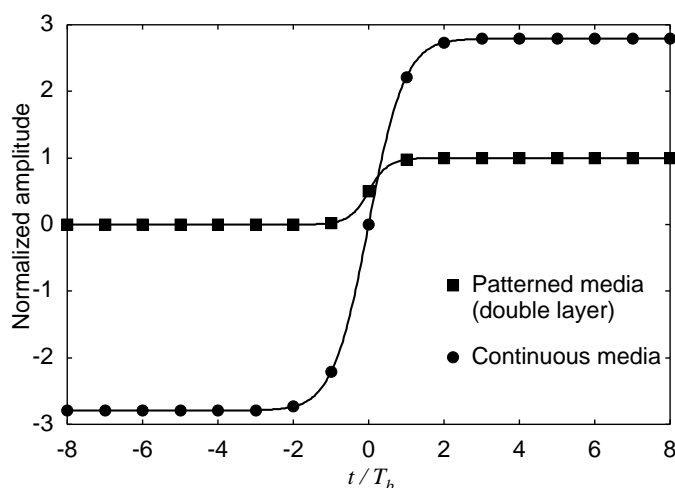


Fig. 9: Isolated waveforms from patterned media and continuous media.

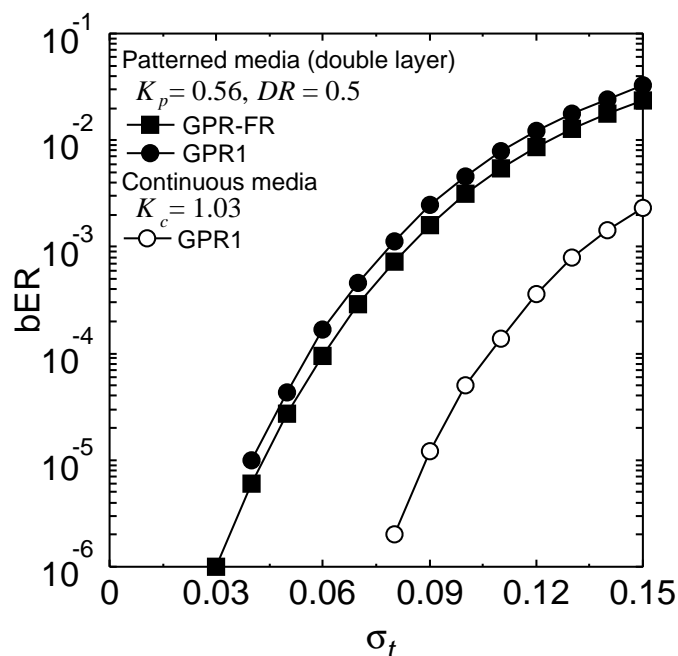


Fig. 10: bER performance ( $\text{SNR}_W=23\text{dB}$ ,  $DR = 0.5$ ,  $x_l = 3.0 \times 10^{-3}$ ,  $x_h = 0.4$ ,  $N_t = 15$ ,  $M = 3$ ).

Table 2: Error Patterns

( $K_p = 0.56, DR = 0.5, K_c = 1.03, x_l = 3.0 \times 10^{-3}, x_h = 0.4, N_t = 15, M = 3$ )

Error pattern	Patterned media	Patterned media	Continuous media
	GPR-FR ML	GPR1 ML	GPR1 ML
$\sigma_t$	0.065	0.060	0.110
bER	$1.64 \times 10^{-4}$	$1.67 \times 10^{-4}$	$1.49 \times 10^{-4}$
0-00	18	16	0
0-01	7	11	0
0-10	8	6	2
0-11	8	5	1
0+00	10	5	20
0+01	16	12	44
0+10	5	6	3
0+11	8	18	1
1-00	10	9	2
1-01	11	13	0
1-10	10	9	43
1-11	16	13	29
1+00	6	10	1
1+01	9	11	1
1+10	8	9	0
1+11	14	10	0

that of the continuous medium.

We analyze error patterns for the PRML channels. All error events were only 1 bit-error in the GPR-FRML channel for the bit-patterned medium. Most of error events are 1 bit-error in the GPR1ML channel both for the patterned and the continuous. Then, we show the error patterns of 1 bit-error in Table II. The character “+” means the error-bit in the case that “0” was reproduced though “1” was recorded. The character “-” shows the opposite case. As can be seen in the table, the number of occurrence for every error pattern is about the same in the bit-patterned medium. In the case of the continuous medium, the number of occurrences depends on the recorded patterns, that is to say, the patterns with transitions at its both sides are dominant, and running tri-transitions is liable to cause decision errors. The recording patterns without transitions hardly cause decision error. Therefore, it can be seen that the bit-patterned medium is efficient in order to cut off the signal dependence of noise.

#### 4. Conclusions

We have studied the approach to find a suitable PRML channels for the R/W channels using bit-patterned media.

The results show that the R/W channel using the double layered patterned medium shows good performance, and the FR channel is suitable for first equalization target for getting good GPR channel. Furthermore, we have discussed the error patterns in the PRML channels. It is clarified that the single bit-error is dominant in R/W channel using the double layered bit-patterned medium as well as the continuous medium and, however, the number of occurrence does not depend on the recording pattern, differently from that of the continuous medium.

#### Acknowledgment

This work is supported in part by the Storage Research Consortium (SRC), Japan.

#### References

- [1] P. W. Nutter, D. McA. McKirdy, B. K. Middleton, D. T. Wilton, and H. A. Shute, "Effect of island geometry on the replay signal in patterned media storage," *IEEE Trans. Magn.*, vol. 40, no. 6, pp. 3551–3558, Nov. 2005.
- [2] G. F. Hughes, "Patterned media write designs," *IEEE Trans. Magn.*, vol. 36, no. 2, pp. 521–526, March 2000.
- [3] S. H. Charap, P. L. Lu, and Y. He, "Thermal stability of recorded information at high densities," *IEEE Trans. Magn.*, vol. 33, no. 1, pp. 978–983, Jan. 1997.
- [4] C. A. Ross, Henry I. Smith, T. Savas, M. Schattenburg, M. Farhoud, M. Hwang, M. Walsh, M. C. Abraham, R. J. Ram, "Fabrication of patterned media for high density magnetic storage," *J. Vac. Sci. Technol. B*, vol. 17 no. 6, pp. 3168–3176, Nov./Dec. 1999.
- [5] P. W. Nutter, I. T. Ntokas, and B. K. Middleton, "An investigation of the effects of media characteristics on read channel performance for patterned media storage," *IEEE Trans. Magn.*, vol. 41, no. 11, pp. 4327–4334, Nov. 2005.
- [6] Y. Suzuki, H. Saito, H. Aoi, H. Muraoka and Y. Nakamura, "Reproduced waveform and bit error rate analysis of a patterned perpendicular medium R/W channel," *J. Appl. Phys.*, vol. 97, 10P108, 2005.
- [7] Y. Suzuki, H. Saito and H. Aoi, "Waveform from patterned perpendicular media," *International Symposium on Ultra-High Density Spinic Storage Systems*, Tohoku University, Sendai, pp. 91–94, July 2005.